DETECTION AND RECONSTRUCTION OF FREE FORM SURFACES FROM AIRBORNE LASER SCANNING DATA

Sagi Filin, Nizar Abo Akel, Yerach Doytsher

Dept. of Transportation and Geo-Information Eng., Technion – Israel Institute of Technology, Haifa 32000, Israel
{filin, anizar, doythser}@tx.technion.ac.il

Commission III, WG 3

ABSTRACT:

Building reconstruction from LiDAR data offers promising prospects for rapid generation of large-scale 3D models in an autonomous manner. Such reconstruction requires knowledge on a variety of parameters that refer to both the point cloud and the modeled building. The complexity of the reconstruction task has led many researchers to use external information, mostly in the form of detailed ground plans to localize the buildings and usually assume that buildings consist of only planar parts. These assumptions limit the reconstruction of complex buildings specifically when curved surfaces exist. We present in this paper a model that considers the point cloud as the only information source and analyzes the roof shapes. We extend the standard models to support free-form surfaces and reconstruct their shape. Since many of the buildings are still composed of planar faces, we maintain the planar based partitioning whenever possible but detect if non-planar surfaces exist and apply free-form surface models there. In such way, the standard models are extended to support general shape roofs without imposing an artificial model if not needed. In addition to the extension into non-planar roofs, our reconstruction involves the aggregation of the point set into individual faces, and learning the building shape from these aggregates. We show the effect of imposing geometric constraints on the reconstruction to generate realistic models of buildings.

1. INTRODUCTION

Three-dimensional reconstruction of buildings becomes a fundamental part in a growing number of applications. Among the data sources available for such reconstruction, airborne laser scanning has emerged in recent years as a leading source for that purpose (see e.g., Brenner and Haala, 1998; Wang and Schenk, 2000; Brenner, 2000; Voegtle et al. 2005; Rottensteiner 2005), particularly due to the direct measurements of the surface topography both accurately and densely.

Reconstruction of buildings from LiDAR data involves their detection in the point cloud, extraction of primitives that compose the building shape, and an agglomeration of the primitives into a geometric building structure. The detection will usually wear the form of object to background separation, e.g., via filtering, surface discontinuities analysis, segmentation, or with the support of external information, like ground plans (Vosselman and Dijkman, 2001; Haala et al. 2006). For the extraction of roof primitives, a segmentation of the data into planar faces will be applied in most cases. In Hoffman (2004) and Alharthy and Bethel (2004) a gradient based analysis is applied as a means to find roof planes. Voegtle et al. (2005) use classified data as an input, where the extraction of the roof planes is region growing based with a homogeneity predicate. Rottensteiner (2005) describes a roof delineation algorithm where the classified data is segmented in a similar fashion as in Voegtle et al. (2005). The boundaries of the detected planes are determined using the Voronoi diagram and the resulting edges are then grouped together into polyhedral models. The reconstruction of the roof model that follows, will usually involve modeling via geometrical representations such as, boundary representations, parametric models, or CSG trees.

Despite the large body of research into building reconstruction, many challenges are still remaining. One such challenge concerns the general planar roof-face assumption that is common to almost all reconstruction models. While planar roof buildings are still the majority, buildings with general shape can be found in almost every scene. Using planar-based models for general curved or free-from surfaces, will lead to a wrong partitioning and a failure in the reconstruction process as the common outcome. Therefore, to increase the reliability of the building detection and modeling process, an extension of the reconstruction model to support a general shapes is a desired improvement. Nonetheless, as many of the buildings are still composed of planar faces, a planar based partitioning is an appealing concept to maintain whenever possible. An optimal reconstruction model will therefore not only involve finding a representation for curved surfaces but also deciding when planarity fails to hold and a more elaborate model is of need.

To support any form of reconstruction that deviates from the planarity assumption, the utility of turning into a curved surface description should be weighted. In this paper, we address the problem of identifying curved roof faces when such exist. The motivation is limiting such detection only to those cases where non-planarity is needed while avoiding over-parameterization elsewhere. We then demonstrate the reconstruction of non-planar roofs structures using data with moderate point density (< 1 p/m^2). In the following Section we outline the roof face extraction model and then describe alternative methods for identifying deviations from planarity by looking into internal and external characteristics. We then study their applicability to the detection of curved segments and show the results of the surface reconstruction.

2. FEATURE EXTRCTION AND MODEL EVALUATION

As noted, a reconstruction framework that assumes no prior information from external sources requires, i) the detection of buildings in the point cloud, ii) segmentation of the roof into faces and analysis of the results, and iii) geometric adjustment

for the building primitives. Our focus here is on the segmentation and segment analysis part. An assumption is made here that buildings have been detected in the point cloud, and that following the roof face extraction and analysis, geometric/topological adjustment of the roof faces will take place.

2.1 Segmentation

Surface segmentation is the core of the primitive extraction process. It is aimed at identifying planar patches in the roof structure, which then allows learning about the roof shape and structure, and reconstructing its shape. The segmentation we apply here is based on cluster analysis that uses local surface parameters as attributes. With those attributes, solid surfaces as roofs tend to cluster as they share slope parameters. Clusters that share common surface properties constitute "surface classes" (all points that share similar surface parameters) that may consist of more than one physical segment. Therefore, following the "surface class" extraction, physical segments in object space are extracted by linking points according to proximity measures. The identified surface segments are validated via surface fitting, which involves testing whether the segment is homogeneous and composed of only one actual plane, and if that is the case, validating that all points in the cluster belong to the same class. The elemental segments are then extended, if possible, by adding unsegmented points and by merging segments that share similar surface properties. Merging of segments is decided by testing whether neighboring segments share similar mean (the estimated surface parameters) and standard deviation. The size of the segments is controlled by *std.* thresholds. An upper bound limit σ_{max} that reflects physical surface accuracy is set to avoid over-segmentation. Additionally a lower bound limit, σ_{min}, which is set in accordance with the expected accuracy of the laser points, is applied to avoid under-segmentation. When a segment is extended and its *std.* falls below the minimum threshold, σ_{min} is used instead.

2.2 Segment Analysis

When planar-surface based models are applied to non-flat surfaces, the reconstruction is likely to provide fractured segments (made of small/narrow) or a sporadic set of patches. From a geometric standpoint, all segments will conform to the segmentation guiding rules like minimum size and adequate *std.* as was defined with the segmentation. Therefore, the decision whether surface patches form a curved face, should not necessarily rely on segment accuracy but rather on internal, or external characteristics.

Internal characteristics – Segments can be considered potential parts of a curved surface if some shape properties indicate so and if the segment does not cover a large area within the building or included within a larger segment (as with dormers, chimneys, etc.). Shape properties can be linked with the arrangement of the offsets among the laser points composing the surface and the adjusted plane. According to adjustment theory, the observations taken should be statistically independent (namely, $E\{\varepsilon_i, \varepsilon_j\}=0 \quad \forall i \neq j$), with E the expectation, and ε, the random errors). Nonetheless, if a plane is fitted to a bended surface, offsets from the plane will tend to cluster and exhibit spatial correlation with offsets of nearby points sharing sign and magnitude. Figure 1.a shows a side view of a curved surface with its corresponding laser points, the

true surface passes among the points with random distribution of points above and below the surface. Figure 1.b shows the segmentation results which led to two planes that approximate the actual surface. As Figure 1.c, shows, the offsets have now some pattern. While the two detected plans have a *std.* that is limited by the segmentation, the residuals do not behave randomly.
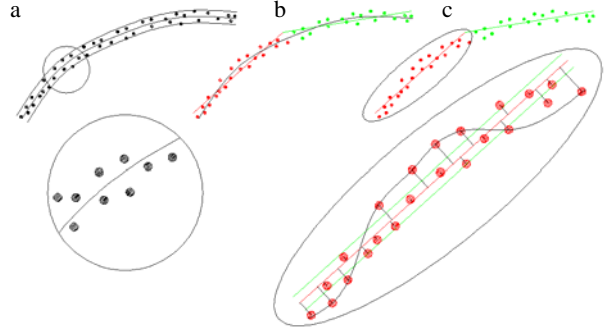

Figure 1: residual analysis, a) curved surface, b) segmentation results, with two planes detected, c) blowup of the left segment showing the spatial order in the residual distribution

Measures to quantify spatial correlation can be found in the literature, e.g., via autocorrelation analysis for time series, or variograms in the two dimensional case. The appealing variogram concept for segment analysis is costly, however, and therefore ineffective. Instead, we turn to non-parametric analysis of the error distribution via a quantitative analysis of the offsets variation. Generally, when a cluster of points will share the same residual sign, each point within this cluster will provide evidence to the non-planarity, and due to the minimum l_2 norm of the least-squares plane adjustment, positive and negative residual regions will be formed across the segment. Therefore, for the evaluation, our hypothesis is that the residual distribution can indicate potential curved segment. To translate this notion into a measure, we analyze the consistency of the residuals signs around a given point, so that

$$p_i = \begin{cases} 1 & \dfrac{\#\left\{\mathrm{sgn}(p_j) = \mathrm{sgn}(p_i)\,\middle|\,p_j \in \mathrm{N}(p_i)\right\}}{\#\left\{p_j \in \mathrm{N}(p_i)\right\}} > t_p \\[2mm] 0 & \text{otherwise} \end{cases} \quad (1)$$

with N the neighborhood around a point p_i within the queried segment and t_p a threshold value that defines the ratio above which a point is considered correlated with its surrounding. Then, a segment is considered curved if $\sum p_i \big/ \# p_i < t_T$, with t_T a threshold ratio. The evaluation of the residual distribution has a very clear dependency on N, the neighborhood function toward which the p_i is evaluated. Filin and Pfeifer (2005) evaluate a set of neighborhood definitions for airborne laser scanning data and opt toward a slope adaptive neighborhood that adapt to a local fitted surface. However, as surfaces are given here by the segmentation, this model has little relevance to the current problem. For neighborhood definition we consider the following set of models:

1. **Euclidean neighborhood** – in which all neighboring points located within a given radius around a point are defined as neighbors, see Figure 2.a.

2. **Topological neighborhood** – in which the topological closest points within the maximal planar graph are considered neighbors. For the graph definition the pointset is triangulated using the Delaunay criterion; see Figure 2.b.

3. **Selective neighbors –** to maintain equal contribution in all direction around the point, a subdivision of the surrounding area is applied. Four quadrants are defined and the closest points in each sector are selected, see Figure 2.c. Around the edges of the segment, where a quadrant partitioning cannot be performed, this approach is maintained, but instead of quadrants the two halves covered by points are evaluated, see Figure 2.d (in narrow segment edge parts this evaluation is not performed, the information that can be drawn there is questionable from the outset).
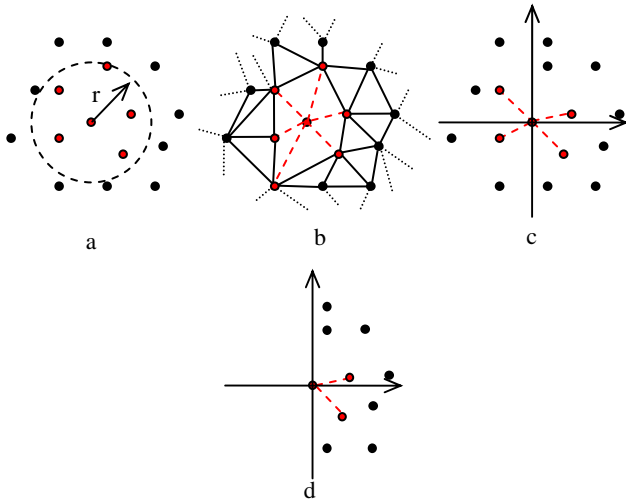
Figure 2. Neighborhoods a) Euclidean, b) topological, c) selective along quadrants, d) selective along edge points

External characteristics – Contrasting the internal characteristics evaluation that studies shape properties via laser points deviation from the surface, the evaluation of external characteristics concerns deciding which segments should be joined together into one curved surface and examining the utility in this. Neighboring planar segments can be grouped together by fitting a high degree parametric surface (e.g., cubic surface), and given the two models deciding which model is preferable. The measure we consider here is the Akaika Information Criterion (AIC) (Akaike, 1974; Boyer et at. 1994) that takes both model complexity and modeling accuracy into consideration, and is advantageous because of its simplicity. Under the reasonable assumption of normal distribution, the AIC values can be computed for each model using Equation (7)

$$AIC \;=\; 2k + n\ln\frac{\sigma}{n} \qquad (2)$$

with k, the number of parameters in the model, n, the number of points, σ, the sum of the square errors. Errors here are the offsets of each point from the surface.

The evaluation is performed in a pair-wise manner, where for each pair of neighboring segments the AIC value is tested for the two individual segments against the merit of using one polynomial surface. Experimenting with polynomial surfaces of degrees 2÷5 has shown that locally, bi-quadratic surfaces (six parameters) are sufficient to decide if the two surfaces are part of a curved surface. The ability to maintain a low-degree polynomial for the test is due to the local pair-wise evaluation. We note that such test can also be applied to evaluate internal characteristics, and refer to it in the following.
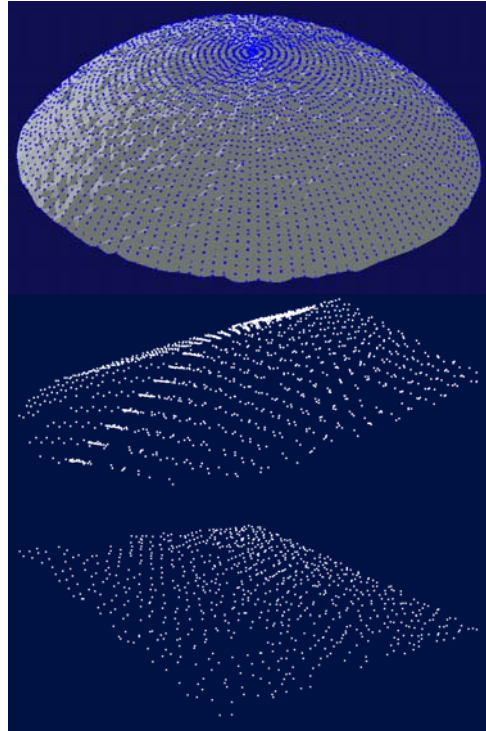

Figure 3: Curved roof datasets, top) a dome like shape, middle) a cross hip roof with curved end, bottom) a nearly flat roof
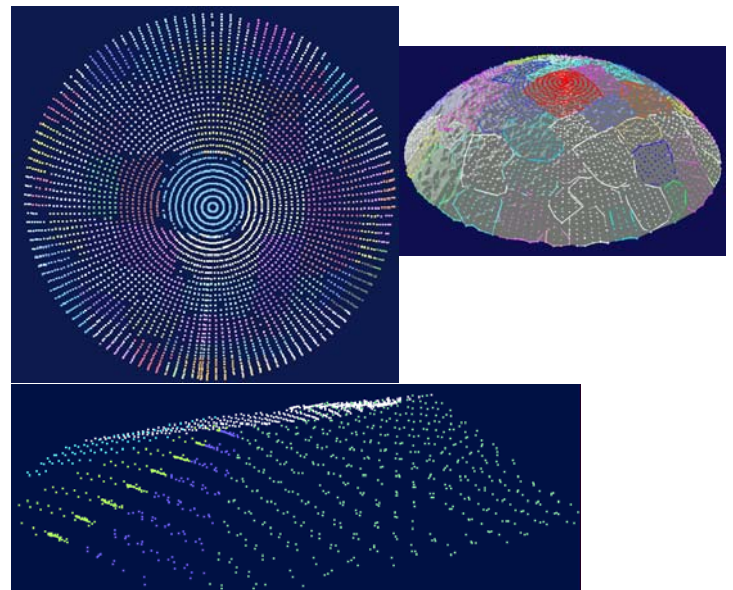

Figure 4: Segmentation results, top) the dome structure with top and isometric view, bottom) the hipped roof

3. RESULTS AND ANALYSIS

For the analysis of the metrics we use three datasets, a synthetic one with a dome like shape (see Figure 3 top), a hip roof with one facet having a cone like shape, (see Figure 3 middle), and a nearly flat roof with no distinct features (Figure 3 bottom), thus making it more challenging for the analysis. The choice of the synthetic dataset is driven the possibility to evaluate the robustness of the proposed methods, particularly to the increase of noise. Noise level ranging from 5 cm as an optimal case to 30 cm as a more extreme end, are applied to study the effect of noise on the surface evaluation model. We study the synthetic and winged roof examples and then analyze the nearly flat roof where further tests are applied. We point that other than the two

Method	Noise: 5 cm		Noise: 10 cm		Noise: 20 cm		Noise: 30 cm	
	Curved	Not Curved	Curved	Not Curved	Curved	Not Curved	Curved	Not Curved
Euclidean	90	2	86	3	74	4	1	57
	97.8%	2.2%	96.6%	3.4%	96.1%	3.9%	1.7%	98.3%
Topological	83	9	40	49	6	71	0	58
	90.2%	9.8%	44.9%	55.1%	7.8%	92.2%	0%	100%
Selective	92	0	88	1	77	0	53	5
	100%	0%	98.9%	1.1%	100%	0%	91.%	8.6%

Table 1. Results of the segment analysis for different noise and neighbourhood methods

real world examples further tests were applied on other building datasets, both flat and free-forms.

The segmentation results for the first two datasets are given in Figure 4. In both cases $\sigma_{max}=\pm15$cm and a minimal segment size of 5 points were used as parameters. For the hipped roof, the two side wings were segmented as planes but the curved parts (the whole structure in the dome, and the front of the hipped roof) are broken into parts. Some holes in the point clouds can be noticed; these are small regions that fell outside the extent of the segments as they exceeded the accuracy threshold, but were too small to form an individual segment. In the overall roof reconstruction scheme, those holes will be "completed" when neighboring planes will be extended to intersect one another. In this regard, because of the actual non-planar shape of the roof, some topological inconsistencies may arise in the reconstruction. We point that for the dome structure some variations in the segmentation as a function of the noise increase can be seen but as they share more or less a similar structure, they are not presented here.
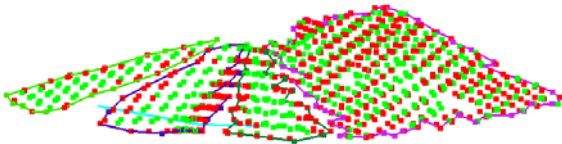

Figure 5: Residual distribution over the individual segments

As for the hip roof, Figure 5 shows the residual distribution over the segments, with green points as positive residuals and red points as negative ones. In all three curved segments a clear clustering of the errors can be notices while the planar roof exhibits more or less random variations.

The application of the internal measures as a means to analyze the shape of the segment is now studied. The results are listed in Table 1 and illustrated graphically in Figure 6. For the experiment, noise level of 5, 10, 20, and 30 cm were applied to the data. For the case of 5 cm noise level all three models appear to perform well, with the Euclidean evaluation having only two misses out of 92 segments and the topological neighborhood giving rise to nine misses from the same amount of segments. The selective neighborhood scheme offers the best performance with no misses at all. As the noise level increases, the dissimilarity in results between the different measures starts growing. The Euclidean neighborhood system offers slight decrease in correct detection up to the 20 cm noise level, but then completely breaks apart at the 30 cm level. This behavior can be attributed to the noise level that exceeds by a factor of two the accuracy threshold of the segmentation. The

topological neighborhood shows a much weaker performance with more the 50% misses already at the 10 cm level and breaking apart from then on. Compared to the two others, the selective scheme appears to have the best performance, with a negligible miss up to the 20 cm level and five misses at the 30 cm level. This result can be attributed to the emphasis on the distribution of the evaluated points while maintaining a proximity criterion to the evaluated point. As Figure 6.b shows those misclassifications occur with the relatively small and narrow segments where the collection of a set of well distributed points is harder.
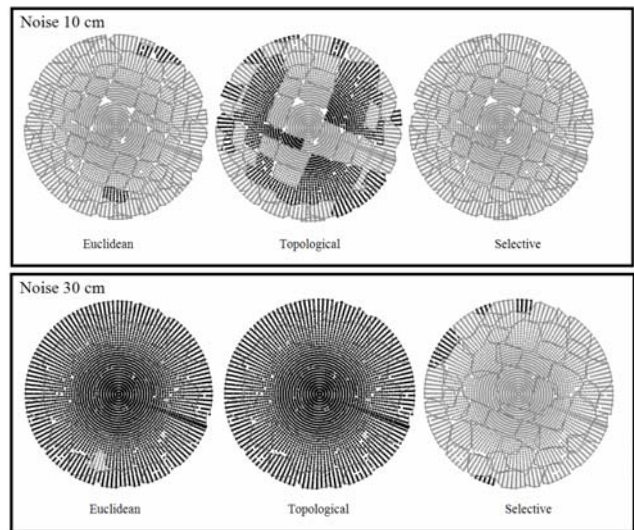

Figure 6: Classification of segment types (light tone – correct, dark tone – wrong)

An analysis of the results leads to the realization that one of the more affecting factors is the size and shape of the evaluated segments. Usually, with curved structures the resulting segments will tend to be small in size, and, depending on the surface geometry, narrow. Therefore, neighborhood models that try covering a relatively broad region, as the Euclidean model or the topological one, will exhibit greater sensitivity to the segment shape and size and as the level of noise increases lose the dominance of the residual distribution. Compared to them, the selective method shows, to some degree, less sensitivity as it weights in both point distribution and proximity in a more controlled manner.

For the segment characterization on the hipped roof the classification results based on the neighborhood systems are listed in Table 2 (for segment numbering see Figure 8).

Generally, both the Euclidean and the selective models classified correctly the three curved related segments, with the topological model misclassifying one of them. The more interesting result however is the classification of the two wing segments, where both the Euclidean and selective based models misclassified one segment. This result is due to the overlap between two different scans over the roof and a systematic scanning error that led to two sets of offsets. In term of the local analysis, it has led both surfaces, under different neighborhood schemes, to be classified as curved.

Method	Segment Number				
	0	1	2	3	4
Euclidean	Flat	Curved	Curved	Curved	Curved
Topological	Flat	Flat	Curved	Flat	Curved
Selective	Curved	Flat	Curved	Curved	Curved

Table 2: Results of the segment analysis for the hipped roof

External evaluation

The external evaluation of the segments' shape operates on a different level by assessing the utility in joining two neighboring segments into a one. The connectivity between the segments is established by identifying border points of each segment (those points that neighbor not only points with the same segment ID but such with others). When applying the AIC measure on the dome structure, the results yield correct classification for all segmentation under different noise levels. The successfulness of the AIC measure can be understood by the direct incorporation of noise level into the information criterion and to the fact that segments that are originally part of a curved object tend to show better results when joined.

When turning to the hipped roof that features both planar and curved part, the model should distinguish between curved parts that should be linked together and planar parts that should be kept as such. Table 3 lists the AIC values for the joining of the roof segments, with Figure 8 showing the resulting connectivity graph between the detected curved segments.

Segment		AIC Values			
I	II	I	II	I + II	curve
1	0	-3102	-3337	-6439	-1675
3		-1002	-3337	-4338	-2125
0	1	-3337	-3102	-6439	-1675
4		-419	-3102	-3521	-1646
3	2	-1002	-1482	-2484	-2688
4		-419	-1482	-1901	-2256
0	3	-3337	-1002	-4338	-2125
2		-1482	-1002	-2484	-2688
1	4	-3102	-419	-3521	-1646
2		-1482	-419	-1901	-2256

Table 3: AIC values - the best model to be selected is the one with the smallest AIC value

The results show that applying the AIC measure when evaluating the utility in joining the three curved segments has managed identifying them as part of a curved segment but when joining the flats with either one another or the curved ones, kept them as they are. We note that the systematic offsets due to the laser strips overlap have no effect on the results as with the

internal characteristics evaluation. This can be explained, again, by the global evaluation of the fitting accuracy and the model complexity that does not evaluate the individual points but rather the merit in joining surfaces.

Figure 8: The connectivity graph between curved segments

Figure 9: Outline of the segments of the nearly flat roof

Turning to the nearly flat surface, the segmentation results are shown in Figure 9. Even though the accuracy level was raised to $\sigma_{max}=\pm25$cm the roof was segmented into two separate segments indicating its actual deviation from planarity. Here, internal measures are measured by the offset based analysis and by using the AIC as a means to assess flatness of the individual segments. Additionally, the external evaluation was performed. As the offsets distribution in Figure 9 show, the bigger segment was indeed classified as curved, but the smaller one as flat. Using the AIC measure to evaluate the two individual segments (flat vs. curved) identified, again, the big segment as curved but the other as flat. This can be explained by the segment size and dimensions that are small and elongated. Contrasting both internal evaluations, the global AIC measure that linked the two parts of the nearly flat roof showed higher gain by joining them into one curved segment. These results indicate that the merit of using the external evaluation lies not only in the information measure, but also in having a more global view of the surface joining utility.

3.2 Global Surface Approximation

Reconstruction of the curved roof shape can be in the form of a high order polynomial or a free-form surface. We demonstrate the application of a Non Uniform Rational B-Spline (NURBS) surface for the reconstruction (Cohen et al., 2001). The results can be seen in Figure 9. Using NURBS allows a mathematical representation that can accommodate and accurately describe surfaces of general shapes, ranging from simple 2D curves to complex 3D free-form surfaces or solids. In addition to the compact representation that NURBS geometry offers, NURBS can be graphically rendered in an efficient and accurate way.

Figure 10 (top) shows that NURBS surface that was fitted to the three curved surfaces, following their boundaries as extracted from the segmentation of the point cloud. Attempting to fit a high order polynomial to the joining of the three surfaces (that appear to be having a cone structure) did not yield satisfying results in terms of appearance and fitting accuracy. The result in Figure 10 (top) that follows the geometric shape of the roof face lacks the form of an actual building shape. In Figure 10(bottom) the application of geometric constraints and leveling the roof boundary is added to form the complete shape of the roof structure. This structure is composed now of two planar and one free-form surfaces. Finally, Figure 11 shows the effect of reconstruction when relying on flat surface based segmentation. It shows the clear role of free-form surfaces for building reconstruction, even for gentle deviations from planarity as the current building offers.
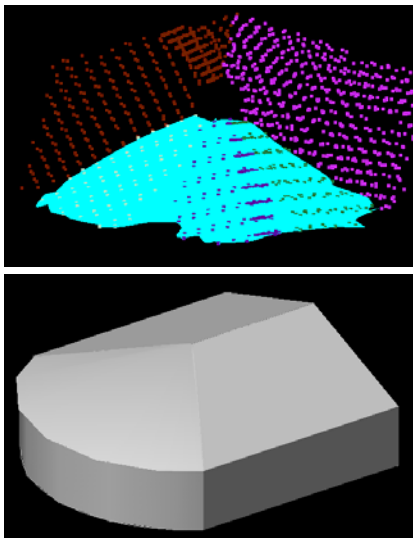

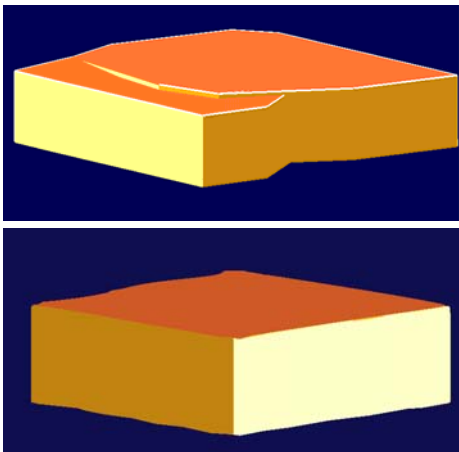**Figure 10**: Reconstruction of the curved part and the roof shape via free-form surface

Figure 11: Reconstructing the nearly flat roof, with an example (top) of the effect of not using a free-form representation

4. CONCLUSIONS

Detection of curved roofs becomes an important component in building reconstruction over large areas, where some buildings are likely to wear such shapes. Such detection should be able identifying them while still maintaining the planarity of other roof faces, which still set the majority. In this paper, we evaluated methods to identify curved surfaces. The results have shown that internal measures can be reach correct detection in most cases under a given neighborhood system. However, the dependency on the segments shape and laser scanning properties, like systematic offsets between strips, may lead to misclassification. In contrast, the external use of AIC criterion appears more robust to noise and to scanning artifacts, as the three examples show. The ability to distinguish correctly between planar surfaces and segments of a fractured curve are of great value in this regard. We note that other external measures may prove suitable as well.

Finally, the application of free-form surface coupled with geometric adjustment of the surface into a building shape has led to an optimal reconstruction of the building model, one that composed of three surfaces for the hipped roof, and of one global surface for the dome and the nearly flat one.

5. REFERENCES

Akaike, H., 1974. A new look at the statistical model identification. *IEEE Trans. on Automatic Control*, **19**: 716-723.

Alharty, A., Bethel, J., 2004. Detailed building reconstruction from airborne laser data using a moving surface method. *Int. Archives of Photogr. and Rem. Sens.***35**(B3): 213-218.

Boyer, K., Mirza, M., Ganguly,G., 1994. The robust sequential Estimator: A General Approach and its application to surface organization in range data. IEEE Trans. on PAMI, **16**(10): 987-1001.

Brenner, C. and Haala, N., 1998. Rapid acquisition of virtual reality city models from multiple data sources. *Int. Arch. of Photogr. and Rem. Sens.* **32**(5): 323-330.

Brenner, C., 2000. Towards fully automated generation of city Boundary points will be clustered at the maximum if they are within a limited spacing and above a certain threshold models. *Int. Arch. of Photogr. and Rem. Sens.* **33**(B3).

Cohen, E., Riesenfeld, R., Elber, G., 2001. Geometric Modeling with Splines: An Introduction. A.K. Peters.

Filin, S., Pfeifer, N. 2005. Neighborhood systems for airborne laser data. *Photogr. Eng. & Rem. Sens.* 71(6): 743-755.

Haala, N., Brenner, C., Anders, K.-H., 1998. 3D Urban GIS from Laser Altimeter and 2D Map Data. International Archives of Photogrammetry and Remote Sensing, **32**(3/1), 339-346.

Haala, N., Becker, S., Kada, M., 2006. Cell Decomposition for the Generation of Building Models of Multiple Scales. International Archives of the Photogrammetry, Remote Sensing and Spatial Information Sciences **36**(3): 19-24.

Hofmann A. D., 2004. Analysis of tin-structure parameter spaces in airborne laser scanner data for 3-d building model generation. International archives of photogrammetry and remote sensing. **34**(B3):302-307.

Rottensteiner. F. 2006, Consistent Estimation of Building Parameters Considering Geometric Regularities by Soft Constraints. *Int. Arch. of Photogr. and Rem. Sens.***36**(3):13-8.

Rottensteiner, F., Trinder, J., Clode, S., Kubik, K., 2005. Automated Delineation of Roof Planes from LIDAR Data. International Archives of the Photogrammetry, Remote Sensing and Spatial Information Sciences **36**(3/W19): 221-226.

Voegtle, T.,Steinlle, E. ,Tovari D. 2005, Airborne laserscanning data for determination of suitable areas for photovoltaics. *Int. Archives of Photogr. and Rem. Sens.* 36(3/W19): 215-220.

Vosselman, G., Dijkman S., 2001. 3D building model reconstruction from point clouds and ground plans. *Int. Arch.s of Photogr. and Rem. Sens.* **34**(3/W4): 37–43.